

High Resolution VSOP Imaging of a Southern Blazar PKS 1921–293 at 1.6 GHz

Z.-Q. SHEN,^{1,3} P. G. EDWARDS,² J. E. J. LOVELL,² K. FUJISAWA,¹ S. KAMENO,¹ and M. INOUE¹

¹ National Astronomical Observatory, 2-21-1 Osawa, Mitaka, Tokyo 181-8588

² Institute of Space and Astronautical Science, 3-1-1 Yoshinodai, Sagamihara, Kanagawa 229-8510

³ Academia Sinica Institute of Astronomy and Astrophysics, P.O. Box 1-87, Nankang, Taipei 115

E-mail(ZS): zshen@hotaka.mtk.nao.ac.jp

(Received March 5, 1999; accepted July 5, 1999)

Abstract

We present a high resolution 1.6 GHz VSOP image of the southern blazar PKS 1921–293. The image shows a typical core–jet morphology, consistent with ground–based VLBI images. However, the addition of data from the space antenna has greatly improved the angular resolution (especially along the north–south direction for this source), and thus allowed us to clearly identify the core. Model fitting reveals an inner jet component ~ 1.5 mas north of the core. This jet feature may be moving on a common curved path connecting the jet within a few parsecs to the 10–parsec–scale jet. The compact core has a brightness temperature of 2.6×10^{12} K (in the rest frame of the quasar), an indication of relativistic beaming. We analyzed the source in terms of three models, involving the inverse Compton catastrophe, an inhomogeneous relativistic jet, and the equipartition of energy between the radiating particles and the magnetic field. Our analysis of this γ –ray–quiet blazar shows no preference to any particular one of these models.

Key words: Galaxies: active — Galaxies: nuclei — Quasars: individual (PKS 1921–293)

1. Introduction

The successful launch of the VLBI Space Observatory Programme (VSOP) satellite HALCA marks a great step forward in increasing the resolution over that possible with ground-based radio telescopes at 1.6 and 5.0 GHz (Hirabayashi et al. 1998 and references therein). HALCA’s 8-meter-diameter antenna is in an elliptical orbit with an apogee of 21,400 km, a perigee of 560 km and an orbital period of 6.3 hours. VSOP observations, with a factor of ~ 3 improvement in resolution compared to the ground observations at same frequencies, enable a close look at the compact core of active galactic nuclei and as a result, to resolve some individual components within the compact core and jets, and to study the bent jet in the vicinity of the core observed at higher frequencies with ground telescopes. In particular, the addition of HALCA significantly improves the north–south resolution for equatorial and southern radio sources, as illustrated in this paper. VSOP also provides almost an order of magnitude increase to the detectable brightness temperature (from 10^{11} – 10^{12} K to 10^{12} – 10^{13} K for bright sources).

As a highly polarized (cf. Worrall, Wilkes 1990) and optically violently variable quasar (Wills, Wills 1981) with $m_v = 17.5$, PKS 1921–293 (OV–236) is classified as

one of the brightest radio–loud blazars known. It shows a dramatic variability from radio to X-ray. Curiously, no γ –ray emission has been detected by EGRET (Fichtel et al. 1994; Mukherjee et al. 1997). At a redshift of 0.352 (Wills, Wills 1981), it has an angular–to–linear scale conversion of $3h^{-1}$ pc mas $^{-1}$ with $H_0 = 100 h \text{ km s}^{-1} \text{ Mpc}^{-1}$ and $q_0 = 0.5$. The existing ground VLBI observations reveal a core–jet structure (cf. Kellermann et al. 1998). Its core is very compact (only a fraction of the beamwidth in diameter), with a brightness temperature (T_b) in the rest frame of the source greater than 10^{12} K. There is evidence that on a scale of 1–2 h^{-1} pc from the core, the jet moves along a curved trajectory superluminally (Shen et al. 1999) and then appears to end up in a diffuse component about $15 h^{-1}$ pc from the core (cf. Tingay et al. 1998).

In this letter, we report on the results of a 1.6 GHz VSOP imaging of PKS 1921–293. We describe the observations and data reduction and present a 1.6 GHz VSOP image of PKS 1921–293 in section 2. The evolution of its fine structure and the implication of the high T_b will be discussed in section 3. A brief summary is given in section 4.

Throughout this paper the spectral index, α , is defined as $S_\nu \propto \nu^\alpha$.

2. VSOP Observations and Data Reduction

The 1.6 GHz VSOP observations of PKS 1921–293 were carried out as part of HALCA’s in-orbit checkout on July 18, 1997 for a total about 1.5 hours. The HALCA data acquisition was successfully done with the satellite tracking stations located in Goldstone (CA, USA), and NRAO¹ Green Bank (WV, USA). The ground radio telescopes consisted of 10 VLBA antennas and the phased VLA of NRAO. The left-circular polarization (LCP) data were recorded in the standard VLBA format with an intermediate frequency (IF) band of 16 MHz. The cross-correlation of the data was carried out on the VLBA correlator at Socorro (NM, USA) with an output preaveraging time of 0.524 and 1.966 seconds for the space-ground and ground-ground baselines, respectively, and 256 spectral channels per IF band.

The post-correlation data reduction was performed in NRAO AIPS and DIFMAP (Shepherd 1997). *A priori* visibility amplitude calibrations were applied using the antenna gain curves and the system temperatures measured at each antenna including HALCA. In the fringe-fitting run, a solution interval of 1 minute and a point source model were employed. The VLBA antenna at Los Alamos (LA) served as the reference telescope throughout. Strong fringes were consistently detected on space baselines to HALCA as well as all the ground baselines. Following this, the data were averaged over all frequency channels, and then phase self-calibrated with a 10-second solution interval and a point source model for the purpose of further time averaging.

Finally, the visibility data were exported to DIFMAP for imaging. The data were integrated over 30 seconds to reconcile the different preaveraging time from the correlator output as mentioned above. The uncertainties in the averaged visibilities were computed from the scatter of data points within the averaging interval. Some obviously bad data were inspected and removed. Several iterations of cleaning and self-calibration to phases (and amplitudes in the later stages) were performed. To ensure a better angular resolution with HALCA data, uniform weighting of the data was adopted with gridding weights scaled by amplitude errors raised to the power of -1 . The resulting image is shown in figure 1. The FWHM beam size is $4.1 \text{ mas} \times 1.1 \text{ mas}$ at a position angle of 46° . (For comparison, the synthesized beam of the ground-only observation is $21.7 \text{ mas} \times 5.7 \text{ mas}$ along -4° .) The peak flux density and the rms noise level are 4.61 Jy/beam and 7.0 mJy/beam , respectively. Thus, a peak-to-rms dynamic range of 650 is obtained in our short 1.6 GHz VSOP image.

Fig. 1. A 1.6 GHz VSOP image of PKS 1921–293 observed at epoch 1997.55 (July 18, 1997) with VLBA and the phased VLA. The restoring beam is $4.1 \text{ mas} \times 1.1 \text{ mas}$ at a position angle of 46° (indicated at the lower left corner). Contour levels are drawn at $-35, 35 \times 1.8^n \text{ mJy beam}^{-1}$ ($n = 0, \dots, 8$), and the peak flux density is $4.61 \text{ Jy beam}^{-1}$.

3. Discussion

3.1. Structural Evolution

PKS 1921–293 was unresolved at arcsecond-scale with VLA observations (Perley 1982; de Pater et al. 1985). Ground VLBI images at centimeter wavelengths showed a typical core–jet structure, with a diffuse jet feature located at a position angle $\sim 30^\circ$ with respect to the compact, strong core (cf. Fey et al. 1996; Tingay et al. 1998; Kellermann et al. 1998). At 43 GHz, three-epoch VLBA images provide evidence for a superluminal jet ($\beta_{app} = 2.1 \text{ } h^{-1}$) within $1\text{--}2 \text{ } h^{-1}$ pc, which has a sharp bend in the position angle compared to the jet seen on a scale of ten parsecs (Shen et al. 1999).

The core–jet morphology of our VSOP image is in good agreement with those ground VLBI images made at other centimeter wavelengths. However, the addition of space VLBI antenna greatly improved the resolution (as can be seen from the comparison of the beams with and without HALCA), and thus enables us to clearly identify the compact core. To yield a quantitative description of the source structure, we applied a model consisting of three elliptical Gaussian components to fit both amplitudes and phases in the calibrated visibility data. The results of model parameters and corresponding $1\text{-}\sigma$ errors are listed in table 1. It reveals that the data are consistent with an inner jet (component 2) at 1.5 mas north of the core (component 1), as well as a large jet feature (com-

¹ The NRAO is operated by Associated Universities Inc., under cooperative agreement with the National Science Foundation

Table 1. Results from Model Fitting to 1.6 GHz VSOP Observation

Component	S (Jy)	r (mas)	θ (°)	a (mas)	b/a	P.A. (°)
1	5.59±0.11	0	0	1.87±0.15	0.38±0.03	48.9±3.4
2	2.03±0.05	1.5±0.2	1.3±4.0	2.70±0.12	0.12±0.01	48.0±3.4
3	4.63±0.10	5.6±0.1	30.4±1.3	3.52±0.14	0.76±0.08	117.8±1.7

Notes – S: the flux density of each component; (r, θ): the distance and position angle of each component with respect to the origin defined by component 1 in mas and degrees, respectively; (a, b/a and P.A.): three parameters of Gaussian component, i.e. major axis (FWHM) in mas, ratio of minor to major axes and the orientation angle in degrees of the major axis

there is still a clear but gradual decrease in amplitude (to ~ 1.0 Jy on the longest baselines of $140\text{ M}\lambda$), which indicates that the compact central part is no longer unresolved. The measured non-zero closure phases on the HALCA baselines also confirm this. The introduction of component 2 is required to fit the visibility distribution at a u - v distance range of $(50 - 70)\text{ M}\lambda$, which is eventually composed of space baselines in the north-south direction. We also tried additional model fitting to visibilities on the space baselines only. This should fit compact core structure well since the extended structure at about 5.6 mas away is totally resolved. The fit gives a separation of two components about 1.6 mas along 3°3, consistent with the results in table 1. We note that component 2 is spatially coincident with an observed 43 GHz weak extended feature of ~ 18 mJy (Shen et al. 1999). If these are the same component at the two frequencies, then the spectral index between 1.6 and 43 GHz would be steeper than -1.6 , which is very common in the optically thin jets. However, since PKS 1921–293 is highly variable, this estimate of spectral index made from measurements taken at different epochs (1.5 years apart) may not be accurate and, further observations are definitely required to clarify this. We found that the position of this inner northern jet component from our 1.6 GHz VSOP experiment with 7 times better resolution in the north-south direction than ground-only VLBI observations (see u - v coverage embedded in figure 2), when compared with those ground VLBI images, is located on a common curved path connecting the jet within $1-2\text{ }h^{-1}\text{ pc}$ to the 10 pc-scale jet.

Fig. 2. A plot shows the model fitting (solid curves) to the visibility amplitude as a function of u - v distance with a plot of u - v coverage embedded.

ponent 3) at a position angle of 30.4° and a separation of 5.6 mas from the core. We note that the orientation angles of the two central components are practically identical, and both are within errors the same as the position angle of the synthesized beam for this observation. We do not regard these coincidences as being physically meaningful, although the model-fitting procedure gives the best results with these values. We are confident, however, that the relative separation and position angle of the components are correct.

We show in figure 2 the distribution of visibility amplitude versus u - v distance along with the visibilities generated from our model fit (solid curves). The plot shows a dramatic drop of the correlated flux density within the ground baselines ($< 30\text{ M}\lambda$), associated with the resolved diffuse jet (component 3) seen in all centimeter ground VLBI images. On the space baselines ($> 50\text{ M}\lambda$),

3.2. Brightness Temperature T_b

PKS 1921–293 has one of the highest brightness temperatures measured in the rest frame of the source. A 22 GHz VLBI survey (Moellenbroek et al. 1996) gave a lower limit to $T_b > 7.0_{-2.1}^{+4.0} \times 10^{12}\text{ K}$ for PKS 1921–293. A previous VLBI experiment, using a telescope in Earth orbit, estimated a core T_b of $3.8 \times 10^{12}\text{ K}$ at 2.3 GHz (Linfield et al. 1989), the highest in the sample for sources with known redshifts. VLBI images made at 5.0 GHz also

found T_b significantly greater than 10^{12} K (Shen et al. 1997; Tingay et al. 1998). The derived core T_b from our 1.6 GHz VSOP image is $(2.55 \pm 0.66) \times 10^{12}$ K, which is consistent with those earlier estimates.

It has been shown that there is a limit to T_b for incoherent synchrotron radiation, and a brightness temperature in excess of this limit is ascribed to the effect of Doppler boosting in a relativistic jet beamed toward the observer with a Doppler factor $\delta = [\gamma(1 - \beta \cos \theta)]^{-1}$ (cf. Readhead 1994). Here $\gamma = (1 - \beta^2)^{-1/2}$ is the Lorentz factor, β is the jet velocity in units of the speed of light and, θ is the angle between the line of sight and the radio jet axis.

A commonly accepted explanation is that the observed upper limit to T_b ($\sim 10^{12}$ K) is caused by the “inverse Compton catastrophe” (Kellermann, Pauliny-Toth 1969). Using formulae (1a) and (1b) rederived by Readhead (1994), we can calculate this inverse Compton scattering limit as $T_{b,ic} = 1.2 \times 10^{11}$ K for PKS 1921–293. Here we have applied a peak frequency of 8.0 GHz and assumed a high frequency cutoff of 100 GHz. The synchrotron self-absorption turn-over frequency of 8.0 GHz was claimed by Brown et al. (1989) and is confirmed by single-dish measurements from the University of Michigan Radio Astronomy Observatory (UMRAO) made around our VSOP observational epoch, from which we also obtained an optically thin spectral index of -0.15 as well as a total flux density of 17.9 Jy at 8.0 GHz. In order to reconcile with $T_b = (1.71 \pm 0.44) \times 10^{12}$ K from our 1.6 GHz VSOP results (here, we have multiplied a factor of 0.67 to convert a brightness temperature derived assuming a Gaussian component to an optically thin uniform sphere), a Doppler boosting factor $D_{ic} = 14.3 \pm 3.7$ is required to avoid the inverse Compton catastrophe. This agrees very well with a lower limit to Doppler factor (δ_{ssc}) of 14 derived from the argument that the observed X-ray emission is produced primarily by the inverse Compton scattering of synchrotron radiation (Güijosa, Daly 1996 and references therein).

The inhomogeneous relativistic jet model (Blandford, Königl 1979; Königl 1981) also sets an upper limit to the measured brightness temperature. This limit is independent of frequency and depends very weakly on the observables with an approximate expression as $T_{b,j} \sim 3.0 \times 10^{11} D_j^{5/6}$ K, here D_j is the Doppler factor associated with this jet model. This results in a $D_j = 12.7 \pm 4.0$, which is very similar to D_{ic} from the inverse Compton catastrophe. Combining with the detected superluminal jet motion $\beta_{app} = 3.0$ (Shen et al. 1999; choosing $h = 0.7$ here), we can derive its bulk Lorentz factor (γ) and the jet angle with the line of sight (θ) as follows: $\gamma_{ic} = 7.5$ and $\theta_{ic} = 1.6^\circ$ from $D_{ic} = 14.3$, and $\gamma_i = 6.7$ and $\theta_i = 2.0^\circ$ from $D_j = 12.7$, respectively. Both models require about the same relativistic beaming factor to explain the high T_b for PKS 1921–293, and we cannot distinguish between them.

Readhead (1994) introduced the “equipartition brightness temperature” cutoff ($\sim 10^{11}$ K) from a statistical analysis. In the case of PKS 1921–293, it gives a limit of $T_{b,eq} = 9.8 \times 10^{10} \delta^{0.78} h^{-2/17}$ K. The 1.6 GHz VSOP core significantly exceeds this limit, and therefore an equipartition Doppler factor as large as $(39.1 \pm 12.9) h^{0.15}$ is needed. This is about 3 times the values of D_{ic} and D_j and suggests that PKS 1921–293 may not be in equipartition. If PKS 1921–293 is not in equipartition, we can use ratio $D_{eq}/\delta = T_b/T_{b,eq}$ with the assumption that δ is about 13 (a value close to D_{ic} , D_j and δ_{ssc}) to derive an equipartition Doppler factor $D_{eq} = (30.6 \pm 7.9) h^{2/17}$, and then $\gamma_{eq} = 14.8$ and $\theta_{eq} = 0.4^\circ$. We can further measure how far the source is from equipartition by calculating the ratio D_{eq}/δ which ranges from $2.2 h^{2/17}$ to $2.4 h^{2/17}$ as δ changes from 14.3 (D_{ic}) to 12.7 (D_j). Güijosa and Daly (1996) obtained a ratio of 2.0 with $D_{eq} = 29$ (assuming $h = 1$). This leads to the conclusion that the core of PKS 1921–293 is strongly particle dominated, since the particle energy density (u_p) greatly exceeds the magnetic field energy density (u_B) by a factor of $(D_{eq}/\delta)^{8.5}$, which is as large as ~ 1000 . Such a departure from equipartition has also been reported for the superluminal blazar 3C 345 (Unwin et al. 1994). We note that both PKS 1921–293 and 3C 345 have not been detected at >100 MeV γ -ray energy in spite of the fact that they are among the strongest blazars at radio wavelengths.

Bower and Backer (1998), in their study of the γ -ray blazar NRAO 530, favor the inhomogeneous jet model which produces a reasonable Doppler factor while maintaining energy equipartition. They also speculate that EGRET-detected blazars are those in which the equipartition limit is briefly superseded by the inverse Compton catastrophe limit. It is also possible that blazars not detected by EGRET may not have equipartition between particle and magnetic field energy densities as in the case of PKS 1921–193 while one of the limits imposed by the inverse Compton catastrophe or the inhomogeneous relativistic jet model applies. In any case, a Doppler factor of 12 is required for PKS 1921–293. This results in a narrow viewing angle $\theta = 1.9^\circ$, at which any small bending angle could be enlarged when projected on the sky. Such phenomenon might be responsible for the observed jet curvature and be further related to its non-detection by EGRET (cf. Hong et al. 1998; Tingay et al. 1998).

4. Conclusions

We have carried out a VSOP observation of the southern blazar PKS 1921–293. The overall source morphology is consistent with previous ground VLBI results. As is clear from figure 2, the space VLBI observations are critical for isolating the core of the source and permit images to be made with much finer spatial resolution than is possible with the ground VLBI at the same frequency. In the

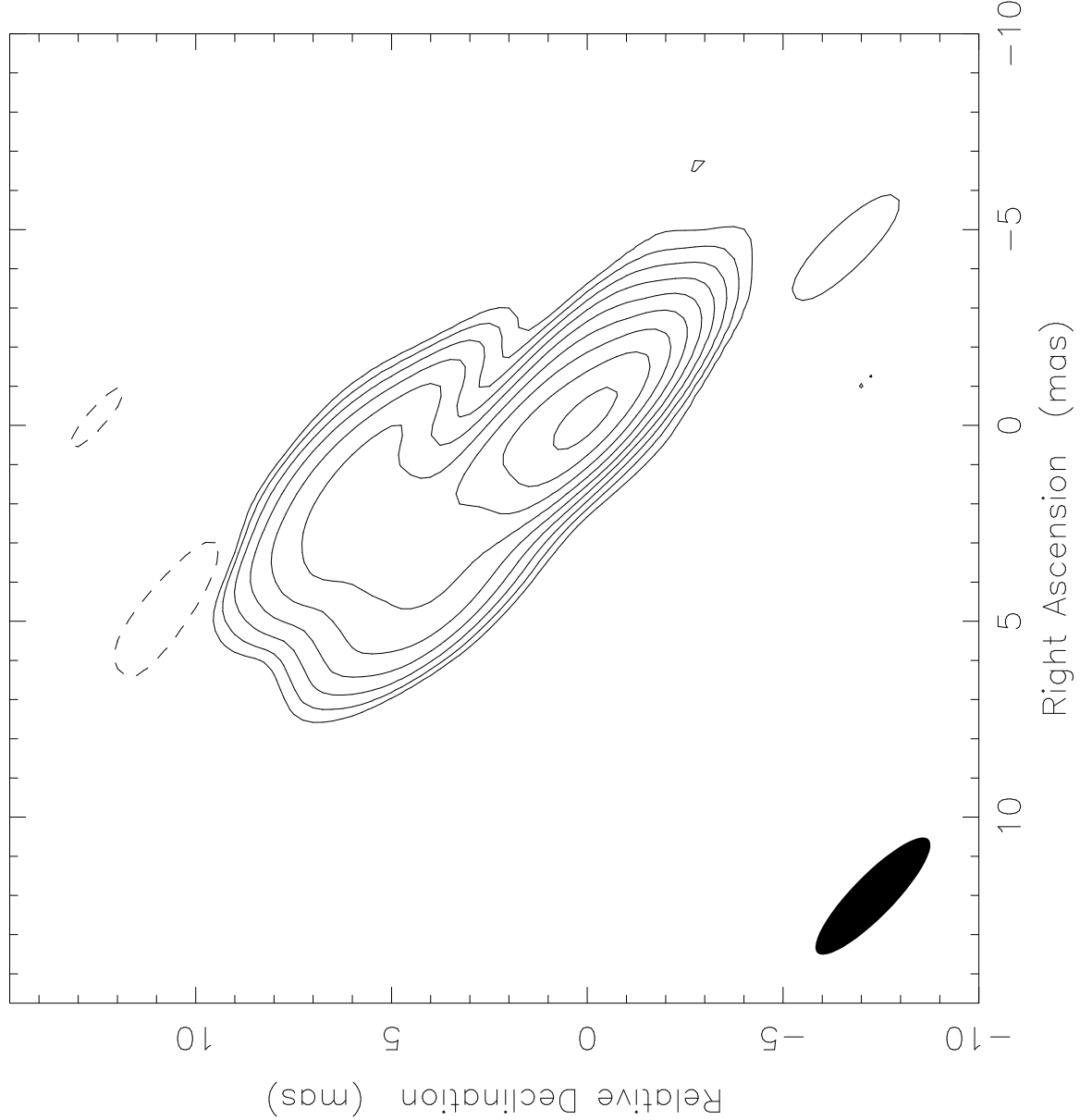
case of PKS 1921-293, the high resolution provided by VSOP data, especially along the north-south direction, plays an irreplaceable role in our resolving an inner jet component at about 1.5 mas north of the compact core. When compared with the ground VLBI images, this feature is believed to relate to the emission on its curved trajectory from the bent jet within $1\text{--}2 h^{-1}$ pc to the 10 pc-scale elongated jets.

By model fitting VSOP calibrated data, we obtain a core brightness temperature of 2.6×10^{12} K in the source rest frame under the assumption that the source has a Gaussian brightness distribution. This is in excess of 10^{12} K, and implies a relativistic beaming in the core. We analyzed the source in terms of three models, involving the inverse Compton catastrophe, an inhomogeneous relativistic jet, and the equipartition of energy between the radiating particles and the magnetic field. We found no significant difference in Doppler factors for first two models, though inhomogeneous jet model is more realistic compared to the homogeneous sphere model in compact radio sources. Both models, however, will eventually lead to a particle dominated departure from equipartition state according to the equipartition argument. Otherwise, a relatively large Doppler factor is needed in order to maintain equipartition of energy in the source. Thus, our analysis of high T_b in this γ -ray-quiet blazar PKS 1921-293 is not in favor of any particular models. More VSOP imaging study of these strong blazars with high brightness temperatures will be necessary to improve our understanding of the physical process within.

We gratefully acknowledge the VSOP Project, which is led by the Japanese Institute of Space and Astronautical Science in cooperation with many organizations and radio telescopes around the world. This research has made use of data from the University of Michigan Radio Astronomy Observatory which is supported by the National Science Foundation and by funds from the University of Michigan. Research at the ASIAA is funded by the Academia Sinica.

References

Blandford R. D., Königl A. 1979, *ApJ* 232, 34
 Bower G. C., Backer D. C. 1998, *ApJ* 507, L117
 Brown L. M. J., Robson E. I., Gear W. K., Hughes D. H., Griffin M. J., Geldzahler B. J., Schwartz P. R., Smith M. G. et al. 1989, *ApJ* 340, 129
 de Pater I., Schloerb F. P., Johnson A. H. 1985, *AJ* 90, 846
 Güijosa A., Daly R. A. 1996, *ApJ* 461, 600
 Fey A. L., Clegg A. W., Fomalont E. B. 1996, *ApJS* 105, 299
 Fichtel C. E., Bertsch D. L., Chiang J., Dingus B. L., Esposito J. A., Fierro J. M., Hartman R. C., Hunter S. D. et al. 1994, *ApJS* 94, 551
 Hirabayashi H., Hirosawa H., Kobayashi H., Murata Y., Edwards P. G., Fomalont E. B., Fujisawa K., Ichikawa T. et al. 1998, *Science* 281, 1825 and erratum 282, 1995
 Hong X. Y., Jiang D. R., Shen Z.-Q. 1998, *A&A* 330, L45
 Kellermann K. I., Pauliny-Toth I. I. K. 1969, *ApJ* 193, 43
 Kellermann K. I., Vermeulen R. C., Zensus J. A., Cohen M. H. 1998, *AJ* 115, 1295
 Königl A. 1981, *ApJ* 243, 700
 Linfield R. P., Levy G. S., Ulvestad J. S., Edwards C. D., DiNardo S. J., Stavert L. R., Ottenhoff C. H., Whitney A. R. et al. 1989, *ApJ* 336, 1105
 Moellenbrock G. A., Fujisawa K., Preston R. A., Gurvits L. I., Dewey R. J., Hirabayashi H., Inoue M., Kameno S. et al. 1996, *AJ* 111, 2174
 Mukherjee R., Bertsch D. L., Bloom S. D., Dingus B. L., Esposito J. A., Fichtel C. E., Hartman R. C., Hunter S. D. et al. 1997, *ApJ* 490, 116
 Perley R. A. 1982, *AJ* 87, 859
 Readhead A. C. S. 1994, *ApJ* 426, 51
 Shen Z.-Q., Moran J.M., Kellermann K.I. 1999, in preparation
 Shen Z.-Q., Wan T.-S., Moran J. M., Jauncey D. L., Reynolds J. E., Tzioumis A. K., Gough R. G., Ferris R. H. et al. 1997, *AJ* 114, 1999
 Shepherd M. C. 1997, in *Astronomical Data Analysis Software and Systems VI*, ASP Conf. Series 125, eds. G. Hunt & H. E. Payne (San Francisco: ASP), 77
 Tingay S. J., Murphy D. W., Lovell J. E. J., Costa M. E., McCulloch P., Edwards P. G., Jauncey D. L., Reynolds J. E. et al. 1998, *ApJ* 497, 594
 Tingay S. J., Murphy D. W., Edwards P. G. 1998, *ApJ* 500, 673
 Unwin S. C., Wehrle A. E., Urry C. M., Gilmore D. M., Barton E. J., Kjerulf B. C., Zensus J. A., Rabaca C. R. 1994, *ApJ* 432, 103
 Wills D., Wills B. J. 1981, *Nature* 289, 384
 Worrall D. M., Wilkes B. J. 1990, *ApJ* 360, 396



1921-293 at 1.648 GHz 1997 Jul 18

